Asian Review of Mechanical Engineering
ISSN: 2249-6289 (P)
Vol.13 No.1, 2024, pp.27-36

www.crijournals.org
DOI: https://doi.org/10.70112/arme-2024.13.1.4238

Development and Characterization of a Remanufactured Motorcycle Clutch Hub from End-of-Life Aluminium Alloy

Efejero Richard Enuwhure, Chinedum Ogonna Mgbemena* and Christopher Okechukwu Izelu
Department of Mechanical Engineering, Federal University of Petroleum Resources, Delta State, Nigeria
*Corresponding Author: mgbemena.ogonna@fupre.edu.ng
(Received 12 March 2024; Revised 17 April 2024; Accepted 26 April 2024; Available online 28 April 2024)

***Abstract* - This study aims to employ reverse engineering in the development of the Yamaha CY 80 motorcycle clutch hub using end-of-life (EOL) aluminium alloy obtained from automotive vehicle scraps. The remanufactured motorcycle clutch hub underwent characterization and transient thermal analysis by integrating the geometric and structural features of the clutch hub. The EOL aluminium was thoroughly washed with a sodium hydroxide (NaOH) solution, cleaned with running water, and dried under sunlight to remove impurities trapped on the metal surfaces. The EOL aluminium alloy was melted in a gas furnace, and the molten metal was cast into the clutch hub using a permanent mold designed with the geometric features and characteristics of the Yamaha CY 80 motorcycle clutch hub. The EOL aluminium alloy was characterized using Fourier transform infrared (FTIR) spectroscopy and scanning electron microscopy-energy dispersive spectroscopy (SEM-EDS). The remanufactured CAD model of the Yamaha CY 80 motorcycle clutch hub was subjected to transient thermal analysis using ANSYS Workbench to predict the thermal behavior of the clutch hub during operation. The FTIR spectra exhibited the following distinctive bands: Al-O stretching modes in octahedral and tetrahedral structures, as well as symmetric bending of Al-O-H, with wavenumbers between 340 and 3131 cm^{-1} for -OH bonds and between 2109 and 1688 cm^{-1} for H-O-H bonds. The SEM-EDS micrographs indicated that the two main elements were bromine and silicon. Results from the transient thermal analysis indicated that the minimum and maximum temperatures were 40.109 °C and 250.09 °C within a time frame of 240 seconds. The maximum total heat flux was 30,271,000 W/m^2. The compressive yield strength and tensile yield strength obtained in this study were 280 MPa, while the ultimate tensile strength was measured at 310 MPa. The alternating stress levels ranged from 62.05 MPa to 275.8 MPa. This study established that the material is susceptible to fatigue failure, as the alternating stress levels were below the material's yield strength of 280 MPa.*
Keywords: **Reverse Engineering, End-Of-Life (EOL) Aluminium Alloy, Transient Thermal Analysis, Fourier Transform Infrared (FTIR) Spectroscopy, Fatigue Failure**

I. INTRODUCTION

In the CY80 Yamaha motorcycle, the clutch hub is one of the 24 components in the clutch assembly that functions as the clutch. These components are enclosed within the clutch basket, as shown in Fig. 1. The clutch hub is made from an aluminium alloy capable of withstanding thermal stresses.

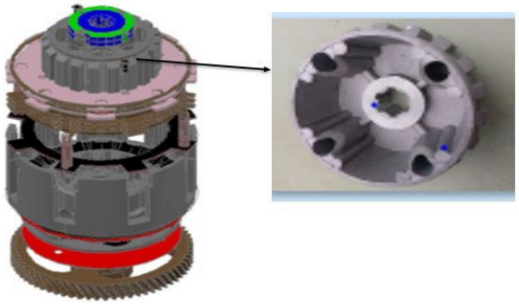

Fig. 1 The CY 80 motorcycle Clutch hub assembly

Several studies have examined the behavior of clutch hubs during service. Patil and Jeyakarthikeyan [1] investigated how mesh size affects the tensile results of clutch hubs. They observed that strain ratios varied with different mesh dimensions and found that the accuracy of finite element method results is directly influenced by mesh shape and size. Liu *et al.,* [3] conducted five finite element analyses and tested the structural strength of the clutch hub, observing that failure occurred in the welding regions. In a different study, ABAQUS and INDEED software were used to examine the structural strength of the clutch hub, with results being fairly similar [4].

Gul *et al.,* [5] assessed the resistance of the clutch disc hub by performing an experimental Charpy test, finding similarities between the FEA-defined clutch hub disc geometry and the experimental Charpy test. Using FEA, torque, and analytical pressure calculations, they evaluated the clutch disc hub's resilience to develop durability hypotheses for real driving conditions. FEA results indicated that the maximum principal stress occurred at the contact points where pressure is applied. These findings were compared to damage locations from bench tests, where cracks and breaks were observed. Post-test damage analysis was conducted to examine fractures. This study allowed for the use of varying hub geometry and different dynamic hub resistance assumptions [6].

Another study proposed a technique for plastic-forming with vibration assistance, examining how this method affects the clutch hub forming process. Experiments were conducted on a hydraulic extrusion press with adjustable vibration frequency and amplitude. When assessing the effect of vibration on forming load and surface quality, both frequency

and amplitude were considered. The results demonstrated that vibration can significantly reduce forming force and improve surface quality [7]. Seung Gyu *et al.,* [8] investigated a drum clutch formed through five processes: first deep drawing, second deep drawing, restriking, embossing, and Grob™. They found that the accuracy of the pre-form significantly influences the finished product's dimensional precision.

The deep drawing, restriking, and embossing techniques used to create the pre-form are critical. Excessive strain during these processes sometimes led to dimensional errors and cracks starting from the product's base and wall. Process factors, such as punch angle, were selected to assess deformation characteristics. The optimal parameters were found using DEFORM commercial FEM codes and the Taguchi method for metal forming simulations. Roll die forming (RDF) was used to manufacture the clutch hub and drum. The material strain field and final product dimensions were analyzed using finite element (FE) analysis. RDF experiments confirmed the dimensional accuracy of the final product. This research demonstrated that RDF can produce a reliable clutch hub [9].

Purohit *et al.,* [10] discussed using SolidWorks Office Premium to design a friction clutch assembly. Static structural analysis was conducted using ANSYS software. The design was iteratively improved based on equivalent stress, total deformation, and factor of safety until a safe design was achieved. The analysis used the uniform wear theory, with cast iron, spring steel, and structural steel chosen for the pressure plate, clutch plate, and diaphragm spring, respectively. The friction material was assumed to be molded asbestos against a cast iron or steel surface. A two- and three-dimensional finite element approach was used to investigate a pressure plate under three main load conditions: thermal loading, centrifugal force, and contact pressure. The findings demonstrated the significance of thermal loading and contact pressure on the design improvement of the pressure and hub plates.

Barve and Kirkire [12] designed a clutch assembly using Pro-E software and conducted a structural study using ANSYS. Modal analysis was used to adjust the natural frequency of the single-plate friction clutch, ensuring it did not resonate with the engine's frequency spectrum. The study showed good agreement between the reduced model and the original model's natural frequencies.

Dhumale and Kamble [13] used CATIA to examine the clutch hub design and performed a static structural analysis using ANSYS. ABS material was used due to its high strength-to-weight ratio, and its performance under high torque was tested. The study demonstrated the effective operation of the clutch hub through static structural analysis. Another study calculated the forces and stresses acting on the clutch and the vehicle's motion to prevent failure under typical conditions. CATIA was used for model design and ANSYS for CAD model simulation [14].

Abdullaha *et al.,* [15] employed the finite element method to numerically simulate the friction clutch system during engagement, assuming no slippage between contact surfaces. Two distinct load situations - contact pressure and centrifugal force - were considered. Numerical calculations were carried out using ANSYS R13. ABS material was used to develop the clutch hub, an engineering plastic chosen for its low production cost and ease of machining. The study established that ABS was effective for producing clutch hubs [13].

According to [10], the pressure plate, diaphragm spring, and clutch plate of the clutch system were made of structural steel, cast iron GS-70-02, and spring steel, respectively. Madhuraj and Bharath [16] recommended using En-GJS-400-15, a ductile cast iron material, as an alternative to the commonly used cast iron alloys, such as FG300 and G2500, for the clutch pressure plate component.

Automotive manufacturing processes employ a wide range of metal-forming techniques. Traditionally, tool design relied on trial-and-error methods and the expertise of die manufacturers. First deep drawing, second deep drawing, restriking, embossing, and Grob™ operations were used to form a drum clutch in five stages [17]. Pre-form accuracy in these stages significantly affects the final product's dimensional accuracy. Excessive strain during these steps can lead to dimensional errors and cracks at the product's base and wall. Commercial finite element codes, such as DEFORM-2D, were used to optimize forming parameters, confirmed through drum clutch forming trials.

Park *et al.,* [17] applied the Taguchi method and FE simulation (FORGE-3D) to identify optimal manufacturing conditions for the drum clutch hub's spline. The significant factors influencing spline development were analyzed, and an experiment was conducted to validate the effectiveness of the optimal settings. Another study examined process variables such as initial blank thickness and punch entrance angle on the clutch hub's cold extrusion process. FE analysis and experiment results demonstrated that optimal parameters can effectively reduce forming load and improve internal spline fillet filling. The cold extrusion process was used to create a clutch outer gear hub [20].

Various methods have been used to cast aluminium alloys, such as centrifugal casting [21]-[23], direct metal casting in permanent molds [24]-[26], squeeze casting [27]-[32], and stir casting [23], [33]-[38]. This study aims to remanufacture a CY80 Yamaha motorcycle clutch hub, characterize the end-of-life (EOL) aluminium alloy used as material, and conduct transient thermal analysis using ANSYS R18.0.

II. MATERIALS AND METHODS

A. Materials

The end-of-life automotive aluminium scraps used in this study were obtained from mechanic workshops and scrap yards in Ughelli, Delta State, Nigeria.

B. Method

The end-of-life automotive aluminium scraps were washed using soap and thoroughly sun-dried before being melted in the furnace.

1. The Permanent Mould Casting: The permanent mold casting of the CY 80 motorcycle clutch hub was accomplished using the steps outlined in Figure 2.

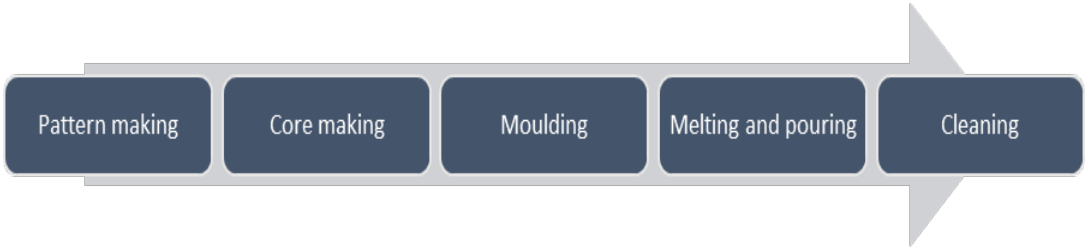

Fig. 2 Metal Casting process

2. Pattern and Core Making: The pattern and core of the mold were made of plaster of Paris, as shown in Figure 3.

Fig. 3 The pattern and core for the clutch hub mould

3. Moulding: The permanent mold is made of brass, as shown in Figure 4. The mold consists of at least two parts: the two mold halves and the cores used to create intricate features.

Fig. 4 The permanent mould made from brass for the clutch hub

4. Melting and Pouring: The melting and pouring were performed in an electrically controlled, gas-fired crucible furnace, as shown in Figure 5.

Fig. 5 Electrically operated gas crucible furnace

C. Material Characterisation

The End-of-Life aluminium alloy was subjected to the following characterization techniques: Fourier Transform Infrared Spectroscopy (FTIR) and Scanning Electron Microscopy-Energy Dispersive Spectroscopy (SEM-EDS).

1. FTIR

The spectra in FTIR of the End-of-Life aluminium alloy were obtained using a Fourier Transform Infrared spectrometer (CARY 630, Agilent Technologies, USA) by thoroughly mixing and pelletizing approximately 10 mg of the End-of-Life aluminium alloy with finely ground KBr to obtain a transparent disc. The pelletized samples were then placed on the IR path. Thirty scans were collected for each measurement in the spectral range of 4000-650 cm-1 at a resolution of 8 cm-1.

2. SEM-EDS

The morphology of the End-of-Life aluminium alloy was observed using a Phenom ProX SEM-EDS (Phenom-World, Eindhoven, Netherlands) with an acceleration voltage of 10 kV and a field of view (FOV) of 537 µm. The surfaces of the samples to be examined were made conductive by palladium-gold sputtering.

D. CAD Design/Model

A model of the CY 80 clutch hub was designed using SolidWorks, with the requisite dimensions measured using appropriate calipers. Figure 6 depicts the CAD model generated with SolidWorks, while Figures 7 and 8 show the dimensions of the remanufactured clutch hub.

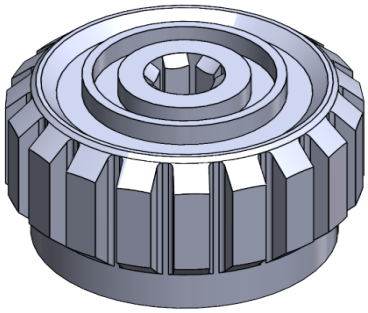

Fig. 6 A CAD Model of the CY80 motorcycle Clutch Hub

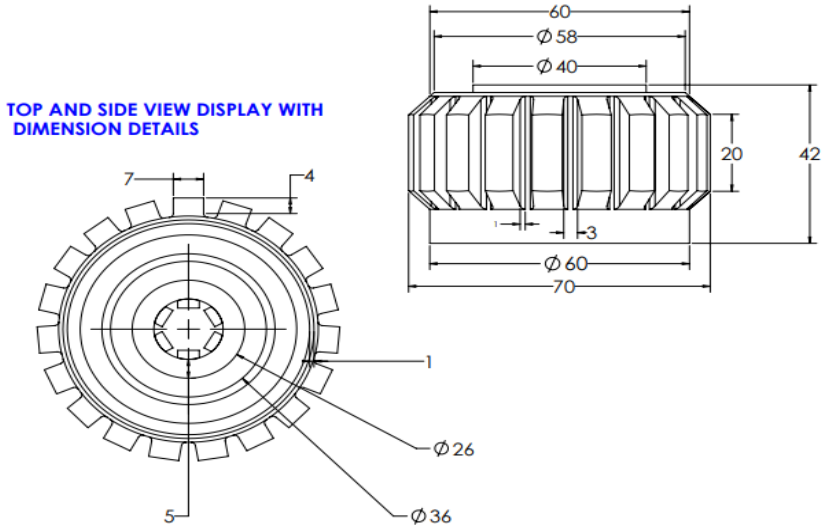

Fig. 7 Detailed Design with Dimensions of the Top and Side views

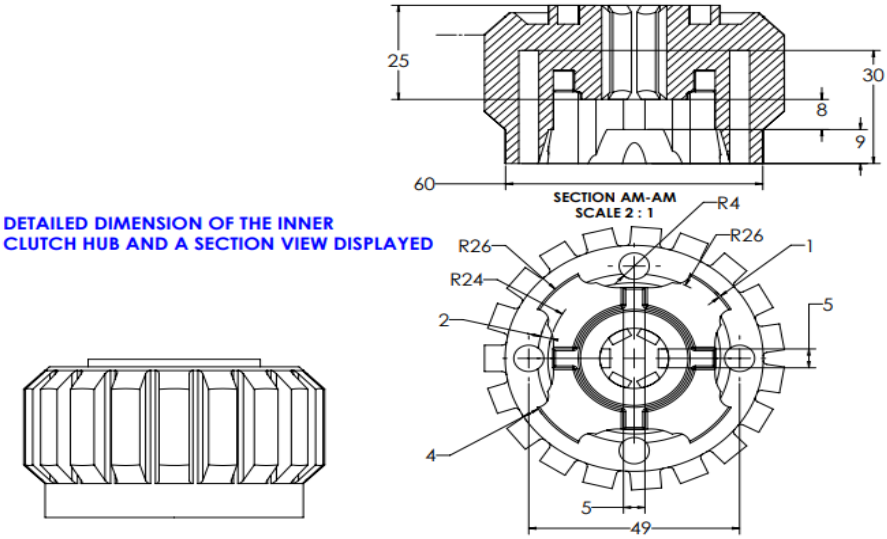

Fig. 8 Detailed Dimensions of the inner clutch hub and a section

E. The Pouring Process

The pouring temperature of aluminium ranges from 650 °C to 700 °C. Before pouring, the mold is properly positioned at the mouth of the furnace. The images of these unmachined clutch hubs are shown in Figure 9.

Fig. 9 The CY80 motorcycle Clutch Hub before machining and finishing

F. Machining

The remanufactured clutch hub was machined to a finish on a lathe machine. Figure 10 shows the machined CY80 motorcycle clutch hub, remanufactured using End-of-Life aluminium alloys from scrap automotive parts.

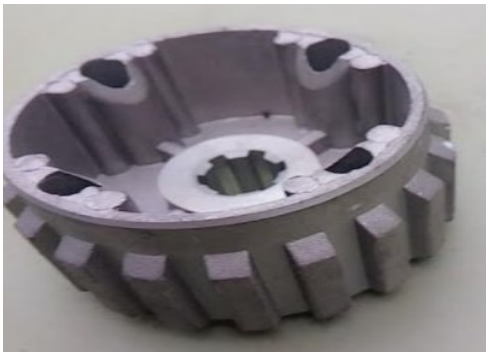

Fig. 10 CY 80 motorcycle clutch hub after machining and finishing

III. RESULTS AND DISCUSSION

A. Fourier Transform Infrared Spectroscopy (FTIR)

The FTIR spectra of the End-of-Life (EOL) aluminium sample are depicted in Figure 11. Thirty scans were collected for each measurement in the spectral range of 4000 to 650 cm^{-1} at a resolution of 8 cm^{-1}. The complete assignment of the absorption bands in the measured IR spectra is summarized in Table I.

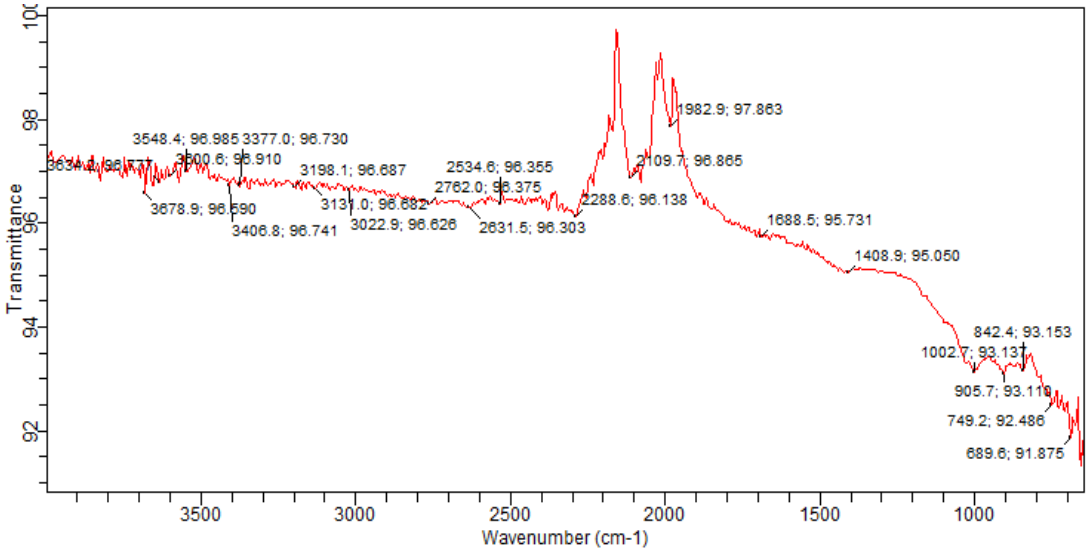

Fig. 11 FTIR Spectra of the Aluminium alloy

TABLE I THE COMPLETE ASSIGNMENT OF THE ABSORPTION BANDS IN MEASURED IR SPECTRA

Assignment	Wave Number (cm^{-1})
-OH bonds	3406-3131
H-O-H bonds$\delta_s Al-O-H$ mode of boehmite and the bands	2109-16881982
$Al-O$ bonds of boehmite	842, 749
$Al-O$ stretching mode in octahedral structure	689
$Al-O$ stretching mode in a tetrahedron and symmetric bending of $Al-O-H$	749-1002

B. Scanning Electron Microscopy Energy Dispersive Spectroscopy (SEM-EDS)

Bromine and silicon were the two main elements observed in the micrograph, as indicated by the SEM-EDS results for the two image scans reported in Figures 12 and 13.

Fig. 12 SEM-EDS for the Aluminium alloy

Element Number	Element Symbol	Element Name	Atomic Conc.	Weight Conc.
35	Br	Bromine	55.61	78.70
14	Si	Silicon	29.32	14.59
9	F	Fluorine	12.76	4.29
27	Co	Cobalt	2.32	2.42

Fig. 13 SEM-EDS for the Aluminium alloy

Element Number	Element Symbol	Element Name	Atomic Conc.	Weight Conc.
35	Br	Bromine	42.08	62.99
14	Si	Silicon	52.06	27.39
38	Sr	Strontium	5.86	9.63

The presence of cobalt in the aluminium alloy improves resistance to hot corrosion and thermal fatigue. Cobalt has a higher melting point than iron and nickel. The inclusion of bromine in aluminium alloys leads to the formation of aluminium bromide, which is used for electroplating aluminium. This process produces a finish that is shiny, thick, adherent, and smooth. Additionally, the incorporation of silicon into aluminium enhances fluidity and lowers the melting temperature, facilitating the manufacturing of castings.

C. Transient Analysis of the CY 80 Motorcycle Clutch Hub

The motorcycle clutch hub design was subjected to transient analysis. The element type selected for the CY 80 motorcycle clutch hub is SOLID186, which was implemented in the ANSYS Workbench program. The 3D model of the CY 80 motorcycle clutch hub was developed using SolidWorks. The 3D meshed model consists of 42,981 nodes and 26,218 elements. The mass and volume of the remanufactured clutch hub are 0.23198 kg and 8.3749e-005 m³, respectively. The initial temperature was set to 22 °C. Table II presents the results obtained for compressive yield strength, tensile yield strength, and tensile ultimate strength of the clutch hub. Figure 14 illustrates the isotropic thermal conductivity of the clutch hub, which increases with an increase in temperature.

TABLE II MECHANICAL PROPERTIES OF THE CLUTCH HUB AFTER TRANSIENT ANALYSIS

Property	Value
Compressive Yield Strength	2.8e+008 Pa
Tensile Yield Strength	2.8e+008 Pa
Tensile Ultimate Strength	3.1e+008 Pa

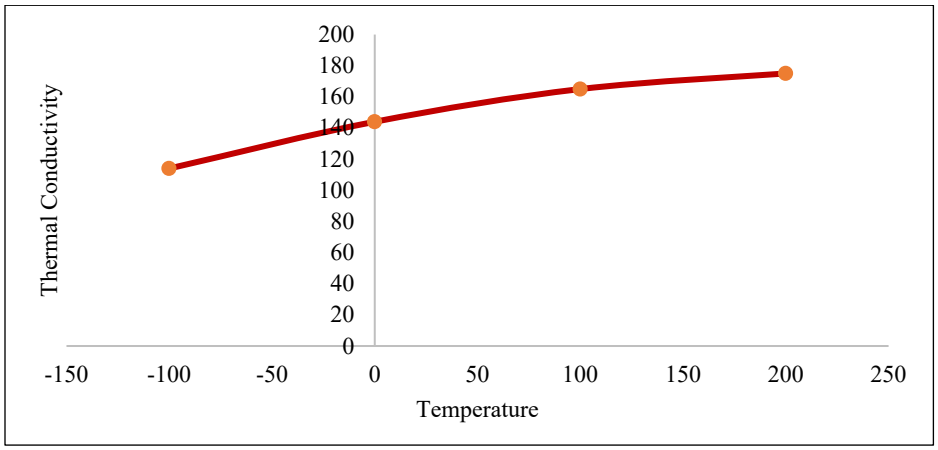

Fig. 14 Isotropic Thermal conductivity

Table III presents the fatigue data for the developed motorcycle clutch hub. A material subjected to alternating stress may experience fatigue failure at stress levels below its yield strength. In spectral loading, the maximum and minimum stresses vary over time and may be arbitrary. Table IV displays the temperature and time scales for the transient thermal analysis conducted on the clutch hub.

TABLE III FATIGUE DATA OF THE MOTORCYCLE CLUTCH HUB

Alternating Stress MPa	Number of Cycles	R-Ratio
275.8	1700	-1
241.3	5000	-1
206.8	34000	-1
172.4	140000	-1
137.9	800000	-1
117.2	2400000	-1
89.63	55000000	-1
82.74	100000000	-1
170.6	50000	-0.5
139.6	350000	-0.5
108.6	3700000	-0.5
87.91	14000000	-0.5
77.57	50000000	-0.5
72.39	100000000	-0.5
144.8	50000	0
120.7	190000	0
103.4	1300000	0
93.08	4400000	0
86.18	12700000	0
72.39	100000000	0
74.12	300000	0.5
70.67	1500000	0.5
66.36	12000000	0.5
62.05	100000000	0.5

The minimum temperature of the transient thermal analysis is 40.109°C, while the maximum temperature is 250.09°C within a time frame of 240 seconds, as indicated in Table IV.

TABLE IV TRANSIENT THERMAL ANALYSIS DATA OF THE CLUTCH HUB

Time [s]	Minimum [°C]	Maximum [°C]
2.4	40.109	250.
3.2	48.915	250.24
3.6403	54.563	250.19
4.0806	60.775	250.17
4.5667	67.874	250.15
5.6573	82.889	250.13
6.9556	97.736	250.11
8.5466	111.2	250.1
10.705	122.96	250.09
13.401	131.49	
16.096	136.33	
18.792	139.21	250.08
21.488	140.82	
24.184	141.73	
26.88	142.24	
29.576	142.54	
32.271	142.7	
40.359	142.85	
64.359	142.91	
88.359	142.92	
112.36		
136.36		
160.36		
184.36		
208.36		
224.18		
240.		

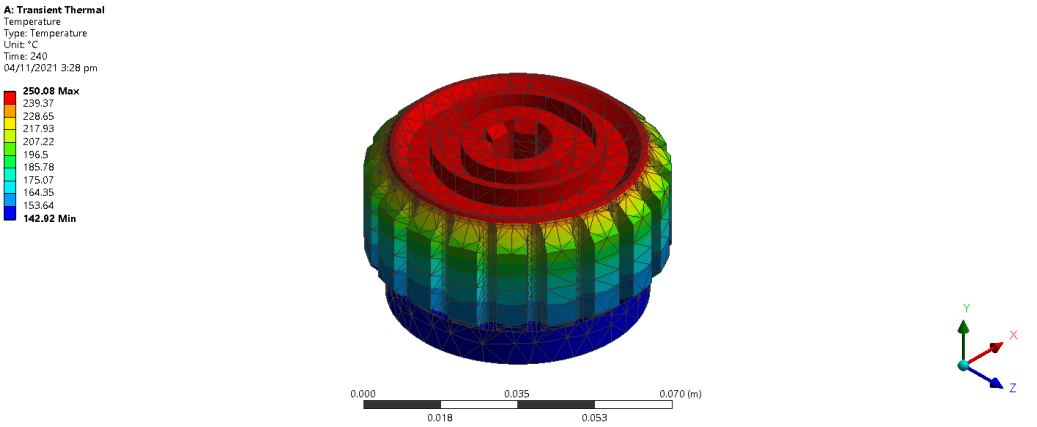

Fig. 15 Temperature Distribution of the Clutch hub (Side view)

Figures 15-17 illustrate the temperature distribution on the clutch hub during the 240-second interval. The figures indicate that the clutch hub developed using End-of-Life aluminium is safe at temperatures below 250°C. The minimum temperature distribution on the clutch hub, as shown in Figures 15-17, is 142.02°C, whereas the maximum temperature is 250.08°C. Figure 18 presents the total heat flux of the clutch hub, with the maximum total heat flux reported as 30,271,000 W/m².

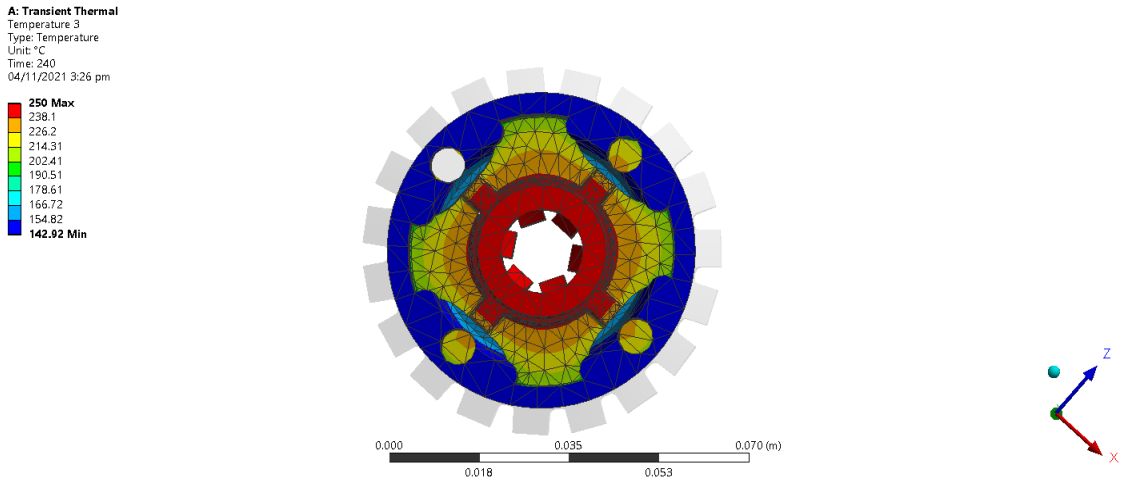

Fig. 16 Temperature Distribution of the Clutch hub (Top view)

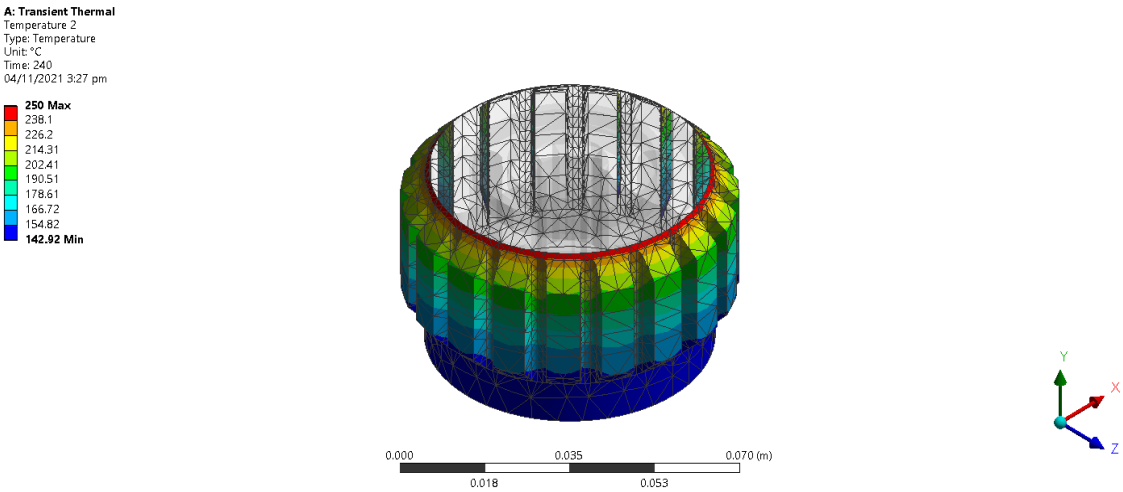

Fig. 17 Temperature Distribution of the Clutch hub (Bottom view)

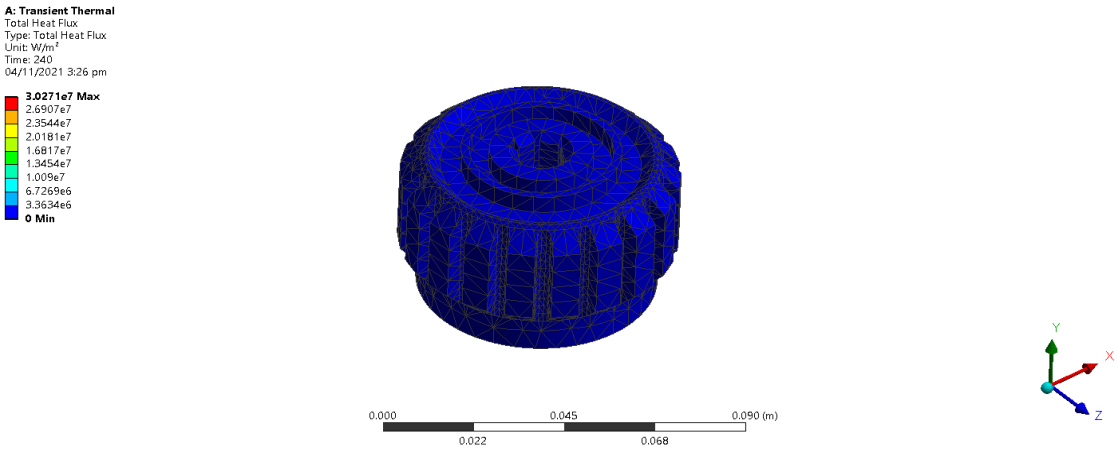

Fig. 18 Total Heat Flux of the Clutch hub

V. CONCLUSION

In this study, several key conclusions were drawn. First, the complete assignment of absorption bands in the measured FTIR spectra, summarized in Table I, revealed characteristic bands, including -OH bonds at wavenumbers ranging from 3406 to 3131 cm^{-1}, H-O-H bonds between 2109 and 1688 cm^{-1}, and Al-O stretching modes at 689 cm^{-1} in the octahedral structure and between 749 and 1002 cm^{-1} in the tetrahedral structure, alongside symmetric bending of Al-O-H. The SEM-EDS micrographs of two image scans, depicted in Figures 12 and 13, showed that bromine and silicon were the predominant elements. In the first scan, bromine had an atomic concentration of 55.61% and a weight concentration of 78.70%, while silicon had an atomic concentration of 29.32% and a weight concentration of 14.59%. In the second scan, bromine's atomic concentration was 42.08% with a weight concentration of 62.99%, and silicon's atomic concentration was 52.06% with a weight concentration of 27.39%. Additionally, fluorine and cobalt were detected in the first scan with atomic concentrations of 12.76% and 2.32%, respectively, while strontium appeared in the second scan with an atomic concentration of 5.85%. For the finite element analysis (FEA) of the CY 80 motorcycle clutch hub, SOLID186 elements were selected and implemented using the ANSYS 19.1 workbench, with the 3D model developed in SolidWorks. The meshed model had 42,981 nodes and 26,218 elements. Compressive and tensile yield strengths were both measured at 280 MPa, while the ultimate tensile strength was 310 MPa. The isotropic thermal conductivity increased with temperature, and despite alternating stresses ranging from 62.05 MPa to 275.8 MPa, they remained below the yield strength, ensuring no fatigue failure. In the transient thermal analysis, the minimum temperature was recorded at 40.109°C, while the maximum reached 250.09°C. On the clutch hub, the temperature distribution ranged from 142.02°C to 250.08°C, and the maximum total heat flux was calculated to be 30,271,000 W/m^2.

REFERENCES

[1] H. Patil and P. V. Jeyakarthikeyan, "Mesh convergence study and estimation of discretization error of hub in clutch disc with integration of ANSYS," *IOP Conf. Ser. Mater. Sci. Eng.*, vol. 402, no. 1, p. 012065, Aug. 2018, doi: 10.1088/1757-899X/402/1/012065.

[2] X. Liu, Y. Wang, L. Zhao, Y. Xing, and H. Guo, "The analysis of structural strength of UD clutch hub assembly," *Appl. Mech. Mater.*, vol. 303-306, pp. 2754-2757, 2013, doi: 10.4028/www.scientific.net/amm.303-306.2754.

[3] X. T. Liu, Y. S. Wang, L. H. Zhao, Y. F. Xing, and H. Guo, "The analysis of structural strength of UD clutch hub assembly," *Appl. Mech. Mater.*, vol. 303-306, pp. 2754-2757, 2013, doi: 10.4028/www.scientific.net/amm.303-306.2754.

[4] C. Liu, X. Liu, H. Hu, and L. Zhao, "Simulation research on structural strength of the hub plate," in *2008 IEEE Int. Conf. Robot. Biomimetics, ROBIO 2008*, pp. 1310-1312, 2009, doi: 10.1109/ROBIO.2009.4913189.

[5] C. Gul, M. O. Genc, and A. Durmus, "Numerical estimating the shock strength of automobile clutch disc hub," in *Proc. of the Sixth International Conference on Advances in Mechanical and Robotics Engineering-AMRE 2017*, Institute of Research Engineers and Doctors, LLC, Dec. 2017, pp. 16-19, doi: 10.15224/978-1-63248-140-5-37.

[6] A. Karaduman, Z. R. Aktaşgil, M. O. Genc, and M. I. Karamangil, "Investigation of clutch hub strength with various geometries under variable torque conditions," *Sigma J. Eng. Nat. Sci.*, vol. 38, no. May, pp. 111-122, 2020.

[7] D. Meng, C. Zhu, X. Zhao, and S. Zhao, "Applying low-frequency vibration for the experimental investigation of clutch hub forming," *Materials*, vol. 11, no. 6, p. 928, May 2018, doi: 10.3390/MA11060928.

[8] Seung Gyu, Y.-C. Park, and J.-H. Park, "Optimization of pre-form for manufacturing of automobile drum clutch hub products using Taguchi method," *J. Korean Soc. Manuf. Process Eng.*, vol. 9, no. 6, pp. 101-108, 2010. Accessed: Jan. 20, 2022. [Online]. Available: https://www.koreascience.or.kr/article/JAKO201007750337635.pdf.

[9] D. H. Ko et al., "Roll die forming process for manufacturing clutch hub in automotive transmission," *Trans. Mater. Process.*, vol. 20, no. 2, pp. 154-159, 2011. Accessed: Jan. 20, 2022. [Online]. Available: https://www.koreascience.or.kr/article/JAKO201111034723735.pdf.

[10] R. Purohit, P. Khitoliya, and D. K. Koli, "Design and finite element analysis of an automotive clutch assembly," *Procedia Mater. Sci.*, vol. 6, pp. 490-502, 2014, doi: 10.1016/J.MSPRO.2014.07.063.

[11] C. Y. Lee, I. S. Chung, and Y. S. Chai, "Finite Element Analysis of an Automobile Clutch System," *Key Eng. Mater.*, vol. 353-358, pp. 2707-2711, Sep. 2007, doi: 10.4028/www.scientific.net/KEM.353-358.2707.

[12] N. A. Barve and M. S. Kirkire, "Analysis of Single Plate Friction Clutch Using Finite Element Method," *Int. J. Adv. Sci. Res. Eng. Trends*, vol. 2, no. 11, pp. 273-276, 2017.

[13] S. G. Dhumale and S. G. Kamble, "Design and Structural Analysis of Clutch Hub Using CAD," *Int. J. Innov. Eng. Sci.*, vol. 6, no. 2, pp. 17-20, 2021, doi: 10.46335/IJIES.2021.6.2.4.

[14] S. Pradhan, B. Biswal, and G. A. Sharma, "Finite Element Analysis of Dog Clutch Plate Using Numerical Methods," *Int. Adv. Res. J. Sci. Eng. Technol.*, vol. 8, no. 8, pp. 612-622, 2021, doi: 10.17148/IARJSET.2021.88101.

[15] O. I. Abdullaha, J. Schlattmanna, and A. M. Al-Shabibib, "Stresses and Deformations Analysis of a Dry Friction Clutch System," *Tribol. Ind.*, vol. 35, no. 2, pp. 155-162, 2013.

[16] H. N. Madhuraj and M. R. Bharath, "Modeling and Simulation of Clutch Pressure Plate Casting Using Alternate Materials," *AIP Conf. Proc.*, vol. 1943, no. 1, p. 020044, Apr. 2018, doi: 10.1063/1.5029620.

[17] J. H. Park, S. G. Kim, Y. C. Park, and X. G. Song, "Shape Design of the Deep-Drawing Preform for Manufacturing of Automobile Drum Clutch Hubs," *Proc. Inst. Mech. Eng. C J. Mech. Eng. Sci.*, vol. 226, no. 4, pp. 1016-1024, Apr. 2011, doi: 10.1177/0954406211417495.

[18] A. K. Khandagale, "Design and Manufacture a Pressure Die Casting Tool for the Manufacturing of the Clutch Hub," *J. Publ. Int. Res. Eng. Manag.*, vol. 5, no. 9, pp. 1-6, 2022.

[19] G. Mahendran, M. A. S. Balaji, D. Dinakaran, and A. Eakambaram, "Optimal Process Parameter Selection for Pressure Die Casting of Clutch Hub Using Desirability Approach," *AIP Conf. Proc.*, vol. 2395, no. 1, p. 040011, Oct. 2021, doi: 10.1063/5.0069968.

[20] Z. Liu, J. Zhou, W. Feng, and Y. Chen, "Modeling, Analysis, and Multi-objective Optimization of Cold Extrusion Process of Clutch Outer Gear Hub Using Response Surface Method and Meta-heuristic Approaches," *Int. J. Adv. Manuf. Technol.*, vol. 116, no. 1-2, pp. 229-239, Sep. 2021, doi: 10.1007/s00170-021-07451-2.

[21] R. Jojith and N. Radhika, "Investigation of Mechanical and Tribological Behaviour of Heat-Treated Functionally Graded Al-7Si/B4C Composite," *Silicon*, vol. 12, no. 9, pp. 2073-2085, Sep. 2020, doi: 10.1007/s12633-019-00294-3.

[22] H. Mahdy, T. Enab, A. Galal, and M. Samuel, "Experimental Study of Manufacturing Aluminium Alloy Pistons Using Vertical Centrifugal Casting Process," *Int. J. Sci. Eng. Res.*, vol. 7, no. 8, pp. 198-203, 2016. Accessed: Sep. 01, 2019. [Online]. Available: file:///C:/Users/edumgbemena/Documents/PISTON_PAPERS/IJSERPaper--I086678---8-2016.pdf.

[23] N. Radhika and R. Raghu, "Characterization of Mechanical Properties and Three-body Abrasive Wear of Functionally Graded Aluminium LM25/Titanium Carbide Metal Matrix Composite," *Materwiss. Werksttech.*, vol. 48, no. 9, pp. 882-892, Sep. 2017, doi: 10.1002/mawe.201700559.

[24] C. O. Mgbemena and I. Emovon, "Fabrication and Assessment of a Motorcycle Piston Using the Traditional Sand Casting Method," *Covenant J. Eng. Technol.*, vol. 4, no. 1, Jun. 2020. Accessed: Aug. 18,

2022. [Online]. Available: https://journals.covenantuniversity.edu.ng/index.php/cjet/article/view/2068.

[25] C. O. Mgbemena and C. E. Mgbemena, "Productization, Characterisation and Analysis of RX 100 Motorcycle Piston from End of Life Aluminium Pistons," *FUPRE J. Sci. Ind. Res.*, vol. 3, no. 2, pp. 44-56, 2019. Accessed: Aug. 18, 2022. [Online]. Available: https://journal.fupre.edu.ng/index.php/fjsir/article/view/62.

[26] S. V. Sujith, M. M. Mahapatra, and R. S. Mulik, "An investigation into fabrication and characterization of direct reaction synthesized Al-7079-TiC in situ metal matrix composites," *Arch. Civ. Mech. Eng.*, vol. 19, no. 1, pp. 63-78, Mar. 2019, doi: 10.1016/j.acme.2018.09.002.

[27] J. Zhu, W. Jiang, G. Li, F. Guan, Y. Yu, and Z. Fan, "Microstructure and mechanical properties of SiCnp/Al6082 aluminium matrix composites prepared by squeeze casting combined with stir casting," *J. Mater. Process. Technol.*, vol. 283, p. 116699, Sep. 2020, doi: 10.1016/j.jmatprotec.2020.116699.

[28] M. F. Alam, "Squeeze casting as alternative fabrication process for carbon fiber reinforced aluminium matrix composites," Ph.D. dissertation, Univ. Ottawa, Ottawa, ON, 2013. Accessed: Sep. 02, 2019. [Online]. Available: https://pdfs.semanticscholar.org/be93/2fbd788197b9983a32bfe8c6e94eb01d772b.pdf

[29] T. R. Vijayaram, S. Sulaiman, A. M. S. Hamouda, and M. H. M. Ahmad, "Fabrication of fiber reinforced metal matrix composites by squeeze casting technology," *J. Mater. Process. Technol.*, vol. 178, no. 1-3, pp. 34-38, Sep. 2006, doi: 10.1016/j.jmatprotec.2005.09.026.

[30] A. K. Singh, S. Soni, and R. S. Rana, "A critical review on synthesis of aluminium metallic composites through stir casting: Challenges and opportunities," *Adv. Eng. Mater.*, vol. 22, no. 10, p. 2000322, Oct. 2020, doi: 10.1002/adem.202000322.

[31] M. Senthil Kumar, R. V. Mangalaraja, R. Senthil Kumar, and L. Natrayan, "Processing and characterization of AA2024/Al2O3/SiC reinforcements hybrid composites using squeeze casting technique," *Iran. J. Mater. Sci. Eng.*, vol. 16, no. 2, pp. 55-67, 2019, doi: 10.22068/ijmse.16.2.55.

[32] A. Ramanathan, P. K. Krishnan, and R. Muraliraja, "A review on the production of metal matrix composites through stir casting - Furnace design, properties, challenges, and research opportunities," *J. Manuf. Process.*, vol. 42, pp. 213-245, Jun. 2019, doi: 10.1016/j.jmapro.2019.04.017.

[33] P. Samal, R. K. Mandava, and P. R. Vundavilli, "Dry sliding wear behavior of Al 6082 metal matrix composites reinforced with red mud particles," *SN Appl. Sci.*, vol. 2, no. 2, p. 313, Feb. 2020, doi: 10.1007/s42452-020-2136-2.

[34] S. Asif, T. Nataraj, and D. V. Rao, "Fabrication, characterization, and finite element analysis of aluminium-based metal matrix composites for automobile clutch hub," *Int. J. Innov. Technol. Res.*, vol. 5, no. 2, pp. 5670-5672, 2017.

[35] C. Fenghong, C. Chang, W. Zhenyu, T. Muthuramalingam, and G. Anbuchezhiyan, "Effects of silicon carbide and tungsten carbide in aluminium metal matrix composites," *Silicon*, vol. 11, no. 6, pp. 2625-2632, Dec. 2019, doi: 10.1007/s12633-018-0051-6.

[36] K. Ravikumar, K. Kiran, and V. S. Sreebalaji, "Characterization of mechanical properties of aluminium/tungsten carbide composites," *Meas. J. Int. Meas. Confed.*, vol. 102, pp. 142-149, May 2017, doi: 10.1016/j.measurement.2017.01.045.

[37] P. Samal, P. R. Vundavilli, A. Meher, and M. M. Mahapatra, "Fabrication and mechanical properties of titanium carbide reinforced aluminium composites," in *Mater. Today: Proc.*, 2019, pp. 2649-2655, doi: 10.1016/j.matpr.2019.07.125.

[38] D. Dey, A. Bhowmik, and A. Biswas, "Effect of SiC content on mechanical and tribological properties of Al2024-SiC composites," *Silicon*, 2020, doi: 10.1007/s12633-020-00757-y.